Conformational Disorder and Ultrafast Exciton Relaxation in PPV-family Conjugated Polymers

Tieneke E. Dykstra,[†] Emmanuelle Hennebicq,[‡] David Beljonne,[‡] Johannes Gierschner,[‡,§] Gil Claudio,[||] Eric R. Bittner,[⊥] Jasper Knoester,[#] and Gregory D. Scholes*[,†]

Lash-Miller Chemical Laboratories, Institute for Optical Sciences and Centre for Quantum Information and Quantum Control, University of Toronto, 80 St. George Street, Toronto, Ontario, M5S 3H6 Canada, Laboratory for Chemistry of Novel Materials, Center for Research on Molecular Electronics and Photonics, University of Mons-Hainaut, Place du Parc 20, B-7000 Mons Belgium, Madrid Institute for Advanced Studies (IMDEA Nanoscience), UAM, Module C-IX, third Level, Av. Tómas y Valiente, 7, Campus Cantoblanco, E-28049 Madrid, Spain, Max Planck Institute for Polymer Research, Postfach 3148 D-55021 Mainz, Germany, Department of Chemistry and Center for Materials Chemistry, University of Houston, Houston, Texas 77204, and Institute for Theoretical Physics and Zernike Institute for Advanced Materials, University of Groningen, Nijenborgh 4, 9747 AG Groningen, The Netherlands

Received: August 13, 2008; Revised Manuscript Received: September 30, 2008

We report combined experimental and theoretical studies of excitation relaxation in poly[2-methoxy,5-(2′-ethyl-hexoxy)-1,4-phenylenevinylene] (MEH-PPV), oligophenylenevinylene (OPV) molecules of varying length, and model PPV chains. We build on the paradigm that the basic characteristics of conjugated polymers are decided by conformational subunits defined by conjugation breaks caused by torsional disorder along the chain. The calculations reported here indicate that for conjugated polymers like those in the PPV family, these conformational subunits electronically couple to neighboring subunits, forming subtly delocalized collective states of nanoscale excitons that determine the polymer optical properties. We find that relaxation among these exciton states can lead to a decay of anisotropy on ultrafast time scales. Unlike in Förster energy transfer, the exciton does not necessarily translate over a large distance. Nonetheless, the disorder in the polymer chain means that even small changes in the exciton size or location has a significant effect on the relaxation pathway and therefore the anisotropy decay.

Introduction

Conjugated polymers are used for applications that capitalize on their semiconductor-like properties, optical properties, and ease of processing.[1] In such applications the interplay between free charge carriers and rather strongly bound excited electronic states is important to understand and to control. For example, in a light-emitting device it is the combination of charge carriers to form a bound state (an exciton), the high yield of photoluminescence from that state, and suppression of energy migration to quenching sites that are important. On the other hand, for photovoltaic applications, the central question deals with the irreversible dissociation of excitons into charge carriers. That process might happen instantaneously upon photoexcitation, or it can occur subsequent to exciton relaxation and migration (perhaps to a trap or interface). Thus, the evolution of photoexcitations over quite a large time span (femtoseconds to hundreds of picoseconds) needs to be understood.

Much of the photophysics of conjugated polymer systems is obfuscated by the structure and organization of the polymer chains.[2−14] It is essential to fully understand the primary steps following photoexcitation in these systems in order to design, tune, and optimize their electro-optical properties. In this paper, we focus on examining the fastest dynamics, those that happen in the first 100 fs or so. This time window has not been deeply explored previously, partly because the necessary incisive experimental probes of ultrafast exciton dynamics are not commonly available, but principally because the excited-state evolution on this time scale tends to be complicated owing to possible entanglements among electronic and nuclear degrees of freedom. Recent work has suggested that such ultrafast energy transfer or relaxation dynamics cause the initial anisotropy to be less than 0.4.[15] We can gain insight into these issues by comparing experimental data to theoretical simulations based on molecularly realistic models.

In systems where there is little disorder (ladder type polyphenylenes, oriented films), excitons can delocalize over large sections of the polymer in the low temperature limit. That is, the excited states are akin to the semiconductor band model.[16] This was demonstrated experimentally for the special case of highly ordered polydiacetylene chains dispersed in a host crystal matrix so as to form an ideal one dimensional (1D) quantum wire.[17,18] In contrast, at room temperature disordered flexible polymers, such as poly[2-methoxy,5-(2′-ethyl-hexoxy)-1,4-phenylenevinylene] (MEH-PPV), exhibit electronic excitations that are (de)localized onto only a few repeat units. Site-selective fluorescence and single-molecule spectroscopic studies have indicated that the excitation of such polymer chains can take on a range of energies depending on the nature of the absorbing conformational subunit/chromophore.[11,19−21] Those experiments reveal that polymers in the PPV family are characterized by

* To whom correspondence should be addressed. E-mail: gscholes@chem.utoronto.ca.
[†] University of Toronto.
[‡] University of Mons-Hainaut.
[§] Madrid Institute of Advanced Studies.
[||] Max Planck Institute for Polymer Research.
[⊥] University of Houston.
[#] University of Groningen.

10.1021/jp807249b CCC: $40.75
Published on Web 12/23/2008

distributions of chromophores along each chain, known as conformational subunits.

To understand these polymers, we think in terms of a hierarchy of structural disorder that dictates the interplay between the electronic π-system and slow intramolecular nuclear degrees of freedom. First, owing to the relatively low energy barrier for small angle rotations around bonds along the backbone of conjugated chains, the chain is broken into conformational subunits.[22−31] It is these conformational subunits that constitute the primary absorbing units. After excitation of a conformation subunit, energy is funneled to lower-energy sites on the chain by electronic energy transfer (EET) prior to emission. Part of the experimental evidence for this energy transfer has been obtained from analysis of the polarization anisotropy decays, which reveal that energy migration occurs over multiple time scales from a few to hundreds of picoseconds.[32−37]

Quantum chemical calculations have endeavored to clarify our understanding of the nature of conformational subunits in conjugated polymers.[38−43] These basic light-absorbing units range in size from 2 to 12 repeat units. Recent work has emphasized why it is difficult to pin down a precise definition of a conformational subunit with respect to torsional disorder,[38,41] because "broken" conjugation is a subjective quantity. Indeed, it does not seem at all appropriate to describe polythiophenes in terms of conformational subunits,[41,44] but for PPV derivatives conformational disorder underpins our understanding of the photophysics—the conjugated polymer is a set of chromophores of differing sizes, energies, and orientations. The picture described by Liu et al. is somewhat conceptually different.[42,43] They describe the conformational subunits in terms of their degree of torsional disorder, so that the red-most absorbing units are those that are the most planar, rather than necessarily the longest. We should stress that, from a theoretical point of view, the choice of the chromophore space chosen for our study has a limited influence, as we deal with the exciton states resulting from the coupling between all segments. Thus, the precise basis set of "chromophores" is not crucial. Account of conformational disorder seems not to be required to simulate absorption spectra of conjugated oligomers because the line broadening due to torsional modes is dominant at room temperature.[45] However, compelling evidence for conformational disorder and conformational subunits as constituent chromophores of the polymer comes from experiments such as fluorescence line narrowing.[46]

The basic characteristics of conjugated polymers are derived from those of conformational subunits. However, for conjugated polymers such as those in the PPV family, these conformational subunits can electronically couple to neighboring subunits, forming subtly delocalized collective states of nanoscale excitons that influence the polymer optical properties.[15,38,39,47−49] In the present work we build on previous studies of conjugated polymer dynamics,[48−57] and we investigate the properties and fate of these states at short times (<100 fs) after photoexcitation to ascertain their possible role in the photophysics of MEH-PPV. On the shortest time scales, we suggest these excitons are somewhat delocalized over a few conformational subunits as a result of intersubunit electronic coupling. Researchers generally expect such delocalized states in organic systems to be short-lived, owing to the likelihood of dynamic relaxation processes that localize excitation onto conformational subunits.[58,59] We calculate ultrafast exciton relaxation in an eigenstate representation in order to interpret ultrafast anisotropy decay processes in experimental data. In the theoretical studies of excitation relaxation we examine individual polymer chains to obtain insights that are obscured in ensemble polarization dependent experiments. We find that rapid decay of anisotropy can occur in single PPV chains as a result of relaxation among exciton states. Interestingly, in the course of these dynamics, the exciton does not translate along a significant length scale, unlike in Förster energy transfer. Nonetheless, the effect on anisotropy is significant. We conclude that the large disorder in the polymer site energies, caused by conformational disorder, plays a deciding role in exciton localization and the initial anisotropy decay.

Theory

To start, we calculate the delocalized, or excitonic, states formed by the electronic coupling among conformational subunits within a PPV chain. The degree to which these states are delocalized compared to the basic chromophore units depends on the distribution of excitation energies of the conformational subunits (sometimes called disorder) and the strength of electronic couplings between them. One needs thus to describe properly the site energies as well as electronic couplings among lowest-lying excited states of the distinct chromophores. Site energies and electronic coupling for each pair of OPV segments were determined using correlated semiempirical quantum-chemical techniques on the basis of the ground-state geometries of the distinct OPV segments. This is justified by the fact that it is the nature of electronic excitations at early time after the excitation, that is, prior to any vibrational relaxation process that is sought. Ground-state geometries were optimized using the semiempirical Austin Model 1 (AM1) technique.[60,61] This method has been successfully applied to similar systems by Rissler et al.[62] and was shown to predict geometric structures in very good agreement with high-level ab initio (MP2/6−31G*) results and X-ray diffraction data.[25,63]

The lowest-lying excited states were then computed on the basis of these geometries by means of the semiempirical Hartree−Fock INDO method[64] coupled with a single configuration interaction (SCI) technique.[65−67] The semiempirical Mataga−Nishimoto potential has been adopted to describe the electron−electron interactions.[68,69] To ensure size-consistency, the CI active space was scaled with the number of carbon atoms by considering all the lowest unoccupied and highest occupied molecular orbitals (MOs) with dominant π character. In applying this procedure, four occupied and four unoccupied molecular orbitals were retained per phenylenevinylene unit. A detailed analysis of the lowest singlet excited states reveals that only the most frontier MOs (i.e., molecular orbitals with significant contribution on the ring *para*-carbons) contribute significantly to the lowest two singlet excited states, with the largest one arising mostly from a simple HOMO to LUMO electronic transition as reported previously.[70]

To account for the detailed chemical and conformational structures of the interacting chromophores, a multipolar representation of the transition dipole moments (atomic transition densities[71]) has been used. Transition densities provide a local map of the transition dipole moment induced by an electronic excitation and can be viewed as a local measure of the amount of electronic reorganization undergone by the system during excitation.[72] Within the distributed monopole model[39] adopted here, electronic coupling factors are thus expressed as a sum over pairwise interactions between INDO/SCI atomic transition densities associated with the relevant excited-state of the interacting chromophores.

The electronic coupling between the *m*th and *n*th excited states localized, respectively, on the chromophore sites "1" and "2"

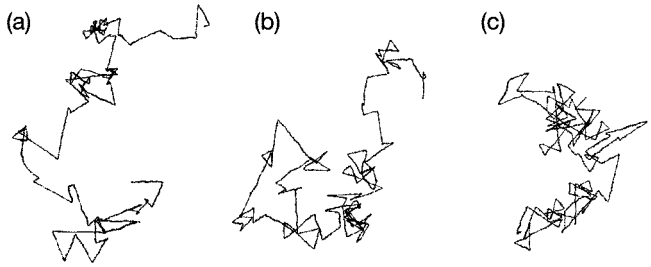

Figure 1. Conformations of three representative chains. The radii of gyration of chains are Chain A: 300 Å, Chain B: 210 Å, and Chain C: 154 Å. The conformations of the chains were generated by MD simulations. The site energies and the couplings between sites were calculated using INDO/SCI techniques.

are expressed in terms of the atomic transition densities over the two chromophores as in the following:

$$V_{1,n;2,m} = \frac{1}{4\pi\varepsilon_0}\sum_a\sum_b \rho^1_{0-n}(a)\rho^2_{0-m}(b)V(a,b) \qquad (1)$$

with $\rho^1_{0-n}(a) = \Sigma_{p\in a}\Sigma_{i,j\in 1}[\sqrt{2}(C^{1,n}_{i,j}c^{1,i}_p c^{1,j}_p)]$ and $\rho^2_{0-m}(b) = \Sigma_{q\in b}\Sigma_{i',j'\in 2}[\sqrt{2}(C^{2,m}_{i',j'}c^{2,i'}_q c^{2,j'}_q)]$ where a and b run over all atomic sites on the first and second OPV segments; and $V(a,b)$ is the Coulomb potential in atomic representation, which is taken here as the Mataga−Nishimoto potential.[68] $\rho^1_{0-n}(a)$ and $\rho^2_{0-m}(b)$ denote the transition densities on atomic sites a and b associated with the $S_0 - S_m$ and the $S_0 - S_n$ electronic transitions in the first and second OPV segments, respectively. $C^{1,n}_{i,j}$ ($C^{2,m}_{i',j'}$) is the CI coefficient weighting the contribution from the monoexcited configuration resulting from a transition between occupied MO i and unoccupied MO j to the nth (mth) singlet excited-state of the first (second) chromophore.

PPV chains were generated using a self-avoiding chain growth scheme parametrized based on ab initio calculations of a small phenylenevinylene oligomer, as described elsewhere.[73,74] These chains were "broken up" into chromophores of conjugated segments separated by large dihedral angles. The cutoff angle was adjusted to give experimentally relevant conjugation lengths. A cutoff of around 55° was typically used. Comparison of different cutoff angles shows that there is little dependence on this value. That is, because all of the chromophores are coupled (and the couplings are included explicitly) there is no discernible difference between one large chromophore with central conjugation break or two smaller chromophores that are strongly coupled. INDO/SCI calculations were performed to determine the site energies of the chromophores and the couplings between them. Chromophores shorter than two repeat units were not included in subsequent calculations because of their high energy.

The conformations of three representative chains are shown in Figure 1. The radii of gyration of these polymer chains are estimated to be 300, 210, and 154 Å according to the equation:

$$R_g^2 = (1/2N^2)\sum_{i,j}(r_i - r_j)^2 \qquad (2)$$

where N is the number of monomers. The sum is over all pairs of monomers, (i,j); and $(r_i - r_j)$ is the distance between monomers i,j. A more detailed study of the conformational disorder and its impact of spectroscopy is reported elsewhere.[38] Energetic disorder in MEH-PPV is mostly due to the presence of a broad range of conformers. The cis-defects present in the chains do not necessarily break the conjugation but instead yield more coiled structures.

We begin with a multichromophoric picture where the basis self-consists of conformational subunits with excitation energies H_{nn} and electronic coupling among them H_{nm}. To obtain the collective exciton states $|\nu\rangle$ in terms of the mixing coefficients λ^ν_n, the secular equations were solved,

$$\sum_n (H_{nm} - E_\nu S_{nm})\lambda^\nu_n = 0 \qquad (3)$$

where the energies (E_ν) are defined relative to the ground-state energy of the aggregate, E_0; matrix elements are $H_{nm} = \langle\phi_m|H - E_0|\phi_n\rangle$; and the overlap integrals are $S_{nm} = \langle\phi_m|\phi_n\rangle \approx \delta_{nm}$. The N exciton states are obtained:

$$\Psi_\nu = \sum_n \lambda^\nu_n \varphi_n \qquad (4)$$

It is in this eigenstate basis that we simulate the absorption spectrum and participation ratio as well as the early time excited-state dynamics. Unless otherwise noted, Greek characters (μ,ν) represent eigenstates and Roman characters (m,n) are chromophores in the site representation.

Simulation of Absorption and Fluorescence. We have simulated the absorption and fluorescence spectra for the single PPV chains using the equations below. High-frequency vibrational modes are included explicitly in the simulation of absorption and emission. They were incorporated using the following equations for the area-normalized absorption and fluorescence spectra:[75−77]

$$a_i(\varepsilon) = \langle\sum_\nu N_a|\mu_\nu|^2\sum_k P(k)\mathrm{Re}\int_0^\infty \mathrm{d}t\langle k|k(t)\rangle \times \exp[i(\varepsilon - \varepsilon^k_\nu - \lambda)t/\hbar]\exp[-g(t)]\rangle\varepsilon/n \qquad (5)$$

$$f_i(\varepsilon) = \langle\sum_\nu N_f|\mu_\nu|^2\sum_k P(k)\mathrm{Re}\int_0^\infty \mathrm{d}t\langle k|k(t)\rangle \times \exp[i(\varepsilon - \varepsilon^k_\nu + \lambda)t/\hbar]\exp[-g^*(t)]\rangle\varepsilon^3 \qquad (6)$$

where $g(t)$ is the line-broadening function that was previously estimated from experiment,[49] the temperature was set to 300 K, λ is the reorganization energy associated with the Stokes' shift, and ε^k_ν is the transition frequency of the νth chromophore adjusted for thermal population of the kth vibrational mode. The spectrum is weighted by the Boltzmann weighting $P(k)$. $\langle k|k(t)\rangle$ is the time-dependent overlap of the initial vibration k with its evolution in the excited state. This overlap gives the time-domain picture of the vibrational absorption spectroscopy, the Fourier transform of which corresponds to the vibrational component of the absorption.[76,77] N_f (N_a) is a normalization constant. The angular brackets are appropriate for ensemble measurements and indicate an ensemble average over many polymer chains. μ_ν is the transition moment vector, given by the vector sum of the site-localized transition dipole moment vectors:

$$\mu_\nu = \sum_{n=1}^{N}\lambda^\nu_n\mu_n \qquad (7)$$

The specific form of the line broadening function, $g(t)$, includes experimentally determined bath fluctuations and coupling magnitudes.[49] It was calculated from the correlation function $M(t) = 200\ \exp(-t/85) + 177\ \exp(-t/1500)$, where the reorganization energies are in cm^{-1} and the time constants are in fs. In the absence of high-frequency modes, eqs 5 and 6 reduce exactly to the standard line shape functions.[78] The coupling of low-frequency vibrational modes to the electronic transition is taken into account through the bath spectral density. Significant low frequency modes include torsional motions in PPV and its derivatives.[53] The time-resolved fluorescence spectra were calculated using a master equation approach described below and eq 6 with $|\mu_\nu|^2$ replaced by the cumulative ground-state population produced by emission from state $|\nu\rangle$.

The inverse participation ratio (IPR) is a measure of the extent of exciton delocalization and was calculated by:[79]

$$L(\varepsilon) = \langle \sum_{\nu} \Delta(\varepsilon - \varepsilon_\nu)(\sum_{n=1}^{N} (\lambda_n^\nu)^4)\rangle/\rho(\varepsilon) \tag{8}$$

where ρ represents the density of states. The IPR ranges from 1, where the exciton is completely localized on a single chromophore, to 0, where the exciton is delocalized over the entire polymer. The average value over the energy range 26 000−30 000 cm^{-1} for the three chains was found to be 0.7, corresponding to a conjugation length of around 7 repeat units for PPV.

Simulations of the Excited-state Dynamics. To examine the ultrafast dynamics of conjugated polymers unobscured by ensemble averaging, we performed theoretical simulations on single PPV chains ($T = 300$ K). The dynamics of delocalized exciton states will be discussed in the basis of an electronic eigenstate representation. It is reasonable to consider the excitons in a delocalized basis because we are only interested in the early time dynamics. The relaxation and equilibration processes we calculate play a role in localizing probability density to discrete conformational subunits, which then serve as the basis for subsequent electronic energy migration by a Förster type mechanism. We examine the dynamics of the exciton relaxation in isolated PPV chains by solving the master equation:

$$\dot{P}_\nu = -\gamma_\nu P_\nu + \sum_{\mu} (W_{\nu\mu} P_\mu - W_{\mu\nu} P_\nu) \tag{9}$$

where γ_ν is the radiative decay rate constant of state $|\nu\rangle$, W are the transfer rates, and P is the population density. This level of treating the exciton dynamics, which focuses solely on the exciton populations, was found to give an accurate description of the exciton dynamics in linear J-aggregates.[80] Initial conditions were determined based on excitation conditions, as described in the Results section, together with calculated dipole strengths. These coupled differential equations are solved numerically, passing from the differential to the integral form of the equations:[81]

$$P_\nu(t) = P_\nu(0)\exp(-W_\nu t) + \sum_{\mu} W_{\nu\mu} \int_0^t \mathrm{d}t' \exp[-W_\nu(t - t')] P_\mu(t') \tag{10}$$

where $W_\nu = \gamma_\nu + \sum_\mu W_{\mu\nu}$, and solving iteratively. The rate was calculated by eq 11, [81−83]

$$W_{\mu\nu} = D(|E_\mu - E_\nu|) O_{\mu\nu} \times \begin{cases} 1 + \bar{n}(E_\mu - E_\nu), & E_\nu > E_\mu \\ \bar{n}(E_\mu - E_\nu), & E_\mu > E_\nu \end{cases} \tag{11}$$

where $\bar{n} = (\exp(\Delta E/k_B T) - 1)^{-1}$ is the mean thermal occupation (Bose−Einstein distribution), and $O_{\mu\nu}$ is the probability overlap between the two states $|\mu\rangle$ and $|\nu\rangle$. Eq 11 satisfies the principle of detailed balance. The bath spectral density is defined as

$$D(\omega) = \omega_0 \frac{\omega}{\omega_c} \exp\left(-\frac{\omega}{\omega_c}\right) \tag{12}$$

for an Ohmic spectral density,[84,85] with ω_0 as the exciton−phonon coupling constant and ω_c as a cutoff frequency. The overlap probability is given by eq 13.

$$O_{\mu\nu} = \sum_{n=1}^{N} |\lambda_n^\mu|^2 |\lambda_n^\nu|^2 \tag{13}$$

In our simulations we take $\gamma_\nu = |\mu_\nu|^2 \gamma_0$, meaning that an average single-chromophore radiative rate, γ_0, is weighted by the oscillator strength (transition dipole moment squared) of the exciton state of interest. γ_0 was set to be 0.0031 ns^{-1}. This corresponds to an excited-state lifetime of ∼700 ps to 1 ns (neglecting nonradiative decay) when excited by a laser pulse. The actual value depends on the microscopic nature of the individual chain. The value of the radiative lifetime has been shown experimentally to be approximately 1 ns in PPVs.[86,87] However, our simulations are insensitive to the specific value of this rate, as we are probing only the early time dynamics where ≪1% of the initial population is lost due to emission. A cutoff frequency $\omega_c = 60$ cm^{-1} was used in addition to an exciton−phonon coupling parameter (reorganization energy) $\omega_0 = 500$ cm^{-1} in the bath spectral density. This spectral density was obtained by approximately matching the Ohmic spectral density to that calculated based on the Brownian oscillator model used for $g(t)$.

For relaxation between states to be efficient, the states must be energetically similar. However, this is not sufficient to ensure relaxation. The relaxation rate is also dependent on the (spatial) overlap probability between two exciton states. That is, spatial extent and close energy are important. A schematic of the energy relaxation is presented in Figure 2. These exciton relaxation calculations are appropriate only for the first ∼100 fs of the dynamics.

Simulation of the Anisotropy. When a system of randomly oriented polymer chains interacts with polarized light, the probability that any chromophore in the ensemble will absorb light depends upon the projection of its transition moment with respect to the polarization of the electric field vector of the incident light. That is, when the sample is excited by polarized light, the transition dipole needs to be oriented (at least partly) in the direction of polarization. This is the initially prepared state; from this distribution of states relaxation will occur. If that relaxation involves a change in transition dipole orientation, then a change of anisotropy is observed in the ensemble.[88,89] We calculated the anisotropy using the following equation which takes into account loss of anisotropy according to a mean angular displacement of transition dipoles[90] for an isotropic ensemble of polymer chains:

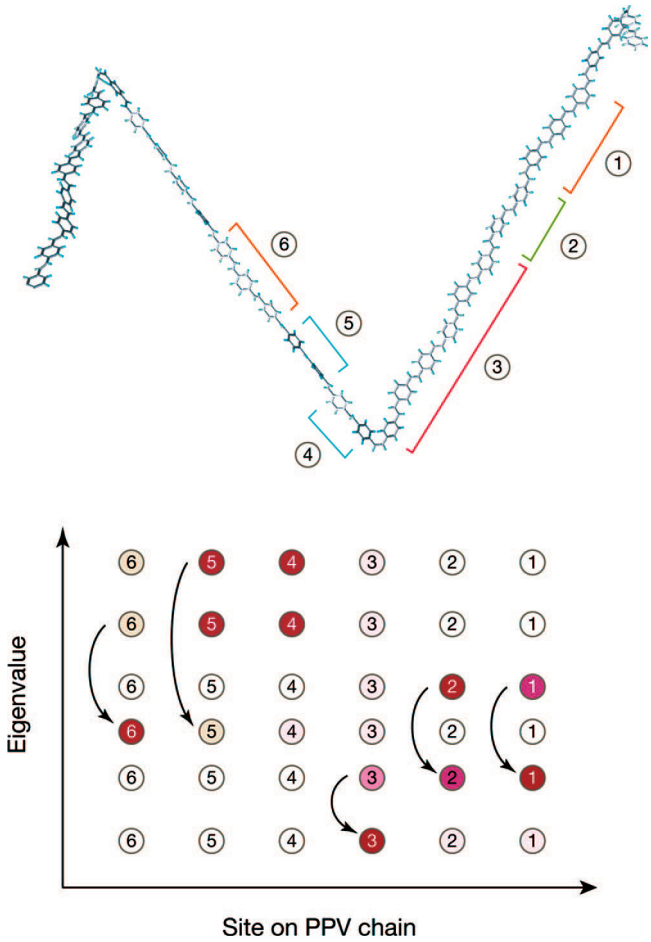

Figure 2. The top panel shows part of a conjugated polymer chain, indicating how torsional disorder effectively breaks the conjugation into a series of chromophores, labeled 1−6. The bottom panel schematically illustrates a series of exciton states formed by interaction among the chromophores 1−6. The depth of color at each site depicts the magnitude of the coefficient for that site in the delocalized eigenstate. For efficient relaxation among states in the exciton manifold, the energies of the two states must be sufficiently similar according to eq 11. The relaxation between states in the exciton manifold is also dependent on the overlap probability between states $O_{\mu\nu}$. When this is included, the relaxation is not simply down the energetic ladder but also depends strongly on the spatial extent of the exciton.[83] The solid arrows indicate transitions that are quick, owing to both energetic and overlap conditions being met.

$$r_0(t) = \frac{1}{5}(3\cos^2\theta(t) - 1) \tag{14}$$

where θ is the angle between absorption and emission transition moments. In the present work we are concerned with anisotropy decay induced by exciton relaxation or exciton migration. To this end, static chains were considered because the rate of rotational diffusion is much slower than the time scale of exciton relaxation. The calculated anisotropy decays correspond to fluorescence anisotropy experiments, not transient absorption.

Because many states may be initially populated by absorption of a laser pulse, a weighted anisotropy is used.[90] This is determined through a coarse-graining approach by calculating the anisotropy decay for each initial condition (where only one state is excited at time, $t = 0$). Then we calculate a weighted average of all of these decays. The weighting is determined by the overlap of the single-state absorption spectrum with the excitation source (the probability that this state would be populated in an ensemble of eigenstates). Those states that are more populated will contribute to the overall anisotropy decay more than the states which have poor overlap. This weighted anisotropy is expressed by eq 15,

$$r_0(t) = \sum_\nu f_\nu r_{\nu 0}(t) \tag{15}$$

where the summation is over all states $|\nu\rangle$ and f_ν is the fractional contribution of the νth state to the absorption.

Experimental Section

One-color pump−probe measurements were carried out as follows. A tunable nonlinear optical parametric amplifier (NOPA) was pumped by 200 μJ of the output of a Ti:sapphire regeneratively amplified laser system that generates ~140 fs pulses at 775 nm and 1 kHz. The tunable visible output of the NOPA was used for excitation.[91] Dispersion was precompensated using a pair of quartz prisms. The laser spectrum was measured using a CVI SM-240 CCD spectrometer. Depending on the laser center frequency, pulse durations of 30−45 fs were obtained from autocorrelation measurements at the sample position. The intensities of the excitation beams were controlled by using a half-wave plate/polarizer combination. Pump and probe beams were synchronously attenuated until the early time signal shape was independent of pulse energy, <5 nJ per pulse at the sample position. The pump and probe are split by a beam splitter with an approximate ratio of 7:3. The probe beam is further attenuated by an Al-coated coverslip by ~200 to 250 times. The probe beam fluence, accounting for its rotation by 45° for simultaneous collection of VV and VH decays, is estimated to be approximately 1/1000th that of the pump. To measure the anisotropy, the pump beam was vertically polarized. The probe polarizer was set to 45°, and a polarization cube before the detectors allowed for simultaneous measurement of the parallel (VV) and perpendicular (VH) signals. The polarization was verified by ensuring that the initial anisotropy for a laser dye was 0.4.

Chlorobenzene (spectroscopic grade) was obtained from Aldrich Chemical Co. MEH-PPV was obtained from American Dye Source. POPV oligomers were provided by H. Meier.[92] Solutions of MEH-PPV or POPV in chlorobenzene were filtered to remove insoluble impurities, and the absorbance was adjusted to be ~0.3 at the absorption maximum in a 1 mm cuvette. The solutions were circulated through a 1 mm path length flow cell using a gear pump. All measurements reported here were conducted at 294 K. To ensure that there was no photodegradation, the absorption spectrum of each sample was compared before and after anisotropy measurements.

Results and Discussion

The absorption spectrum of MEH-PPV in chlorobenzene solution is plotted in Figure 3a together with the three laser excitation spectra used in our experiments. Examples of VV and VH polarized pump−probe transients for MEH-PPV in chlorobenzene solution are provided in the Supporting Information. The polarization anisotropy, defined as[88,90]

$$r(t) = \frac{I_{VV}(t) - I_{VH}(t)}{I_{VV}(t) + 2I_{VH}(t)} \tag{16}$$

is plotted in Figure 3, panels b and c. Figure 3b shows that the measured anisotropy decay depends quite sensitively on laser

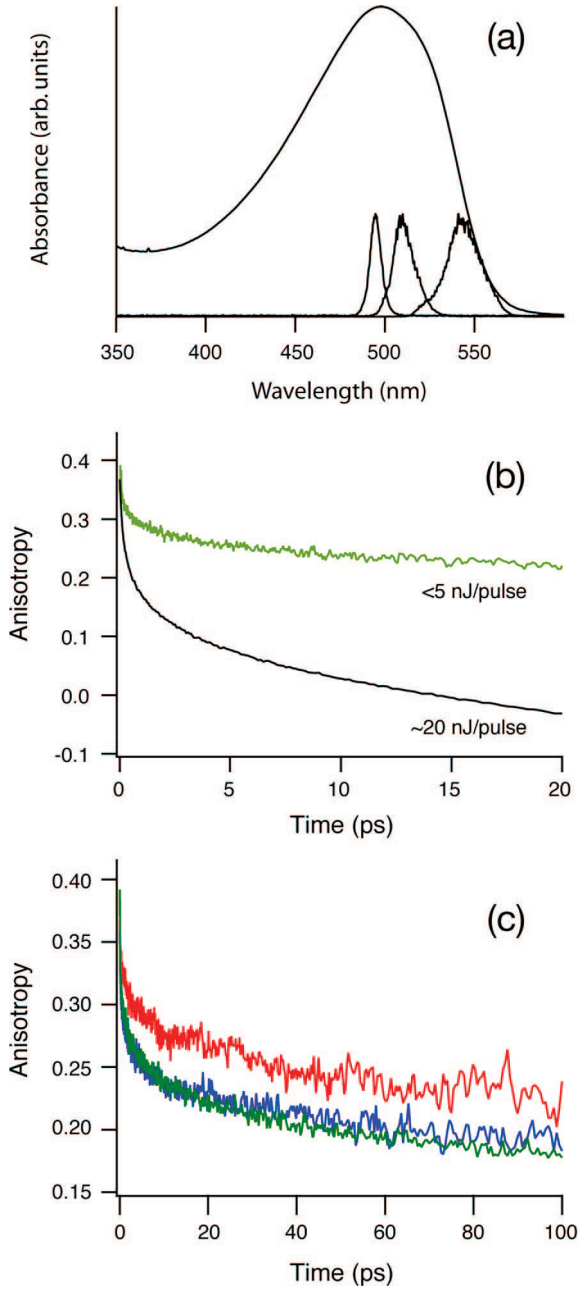

Figure 3. (a) Absorption spectrum for MEH-PPV in chlorobenzene solution. The normalized laser spectra are also shown, with center wavelengths of 493, 510, and 540 nm. (b) Pump−power dependence. Excitation wavelength was 493 nm. (c) Experimental pump−probe anisotropy of MEH-PPV in dilute chlorobenzene solution. Pump/probe wavelengths were 540 nm (red curve), 510 nm (green curve) and 493 nm (blue curve).

power. The fast transient present at moderate excitation energies is attributed to exciton−exciton annihilation.[93] At such excitation intensities, there is a reasonable probability that two or more excitons may occur on the same polymer chain, encounter each other, and annihilate. Multiexciton states are generally short-lived in polymers and other macromolecules because excitations on nearby but distinct chromophores annihilate very effectively, forming a higher electronic state that rapidly relaxes through internal conversion.[94,95] This rapid relaxation is observed in the high intensity anisotropy decay shown in Figure 3b. Care must be taken to avoid such power-dependent effects if one hopes to investigate the dynamics of single excitons.

At sufficiently low excitation pulse energies (<5 nJ/pulse) we found the anisotropy decay profile to become insensitive to excitation intensity, and all further experiments were carried out under those conditions. Thus, we report data in the third-order nonlinear optical regime with minimal exciton−exciton annihilation. Figure 3c demonstrates the excitation wavelength dependence of the anisotropy decay of MEH-PPV in chlorobenzene as measured by one-color pump−probe. Excitation wavelengths were 540, 510, and 493 nm. Care must be taken when interpreting the data at excitation/probe energies higher than the red-edge of the absorption band. These measurements probe a subensemble of population at increasing delay times that includes population that has not undergone EET to lower energy subunits.

We are interested in understanding the fast decay dynamics, so we first need to explain clearly how the pump−probe anisotropy experiment works as a third-order nonlinear spectroscopy. The change in probe intensity (i.e., the intrinsically heterodyned third-order nonlinear optical signal) as a function of pump−probe delay t_p for an optically thin sample of path length l, concentration of absorbers c, and refractive index n is:[78]

$$I_{p-pr}(t_p) \propto \frac{cl}{n}\int_0^\infty dt\ \mathrm{Im}[E^*_{pr}(t_p)\cdot\langle P^{(3)}(0,t_p,t)\rangle]_{\Sigma(\Delta\tau)} \quad (17)$$

where $E_{pr}(t_p)$ is the electric field of the probe pulse, * means complex conjugate, and the subscript $\Sigma(\Delta\tau)$ means that integrations over the finite pulse durations are carried out in such a manner that response functions accounting for nontime ordered pulse sequences are correctly accounted for (e.g., to reproduce the coherence spike). That summation over finite pulse duration can be carried out in conjunction with rotational averaging with respect to the pump−probe polarization to yield a weighted sum over nonlinear response functions:

$$\langle P^{(3)}(0,t_p,t)\rangle = \sum_\alpha a_\alpha(t_p)C^{(4)}_\alpha R_\alpha(0,t_p,t) \quad (18)$$

where a_α is an amplitude denoting the contribution of response function R_α at each pump−probe delay (it depends on pulse duration). $C^{(4)}_\alpha$ relates the laboratory frame pump and probe pulse polarizations to the dipole transition moments of the molecules being photoexcited.[88,89,96−99] For randomly oriented molecules this relationship is governed by an isotropic Cartesian tensor.[100,101] $C^{(4)}_\alpha$ needs to be evaluated for each of the two pump−probe polarization configurations, see Appendix B of ref 102. We wish to point out that the anisotropy decay can be retrieved even during the pulse duration because the sum over response functions cancel in Eq 16, except for the factor that gives the time dependence of the ensemble-averaged transition dipole randomization:

$$r(t) = \left(\frac{\frac{1}{5}-\frac{1}{15}}{\frac{1}{5}+\frac{2}{15}}\right)\langle P_2(\hat{\mu}(0)\cdot\hat{\mu}(t))\rangle \quad (19)$$

The prefactor is equal to 0.4, and the latter factor represents the projection of the transition dipole unit vector rotational correlation function, where $P_2(x)$ is the second-order Legendre polynomial. It is notable that the coherent spike (nontime ordered response functions during pulse overlap[103]) has little effect on the anisotropy, except in special cases, because it is removed by taking the ratio.

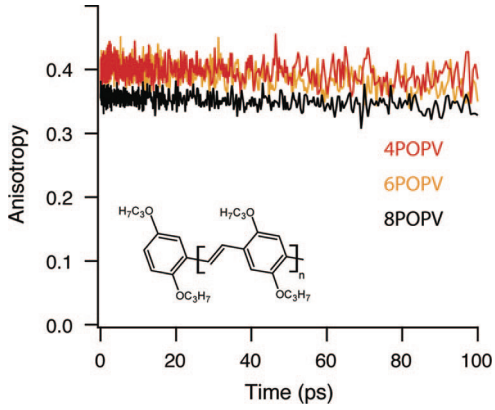

Figure 4. Experimental POPV oligomers' anisotropy decay for n = 4, 6, and 8. Excitation wavelength was 493 nm. Initial anisotropies are approximately 0.4 for 4POPV and 6POPV. The initial anisotropy is slightly lower for 8POPV. The structure is shown as an inset.

Although we focus our discussion on excitons, polaron pairs (or charge transfer excitons) can be a byproduct of the breaking up of initially created excitons.[94,104−113] Polaron pairs are species where the electron and the hole are on different conformational subunits but are still bound. It is possible that some are photogenerated directly, but the consensus is that they are formed in small yield on the time scales we focus on in this work.[114−117] So, although we specialize our discussion to exciton relaxation, which is thought to be the dominant species formed immediately upon ultrafast excitation of MEH-PPV in solution, a contribution to the dynamics from polaron pair formation cannot be discounted.

The initial anisotropy of MEH-PPV in dilute solution was found to be 0.36 ± 0.01 for the pulse duration used in our experiments. The anisotropy decays rapidly during the first ~200 fs, after which it assumes a significantly slower decay profile that accounts for most of the anisotropy decay. Other researchers also consistently record initial anisotropies less than 0.4.[15,32,35] We attribute the low initial anisotropy to a combination of processes that rapidly decay the anisotropy within the finite pulse duration of our experiments. In the simplest treatment of the nonlinear response functions, 0.36 represents an average anisotropy over approximately the first 20−30 fs. We have examined this in more detail using simulations and experiment in other work in our laboratory, and those results substantiate the general idea of this explanation.[118]

The anisotropy decays for a series of POPV oligomers are plotted in Figure 4 for comparison. These data show no anisotropy decay, which implies that dynamics that are intrinsic to the chromophores, such as cooling of torsional mode excitations, segmental motion, or other structural deformations do not contribute to the ultrafast anisotropy decay we observe for the polymer. Note also that the initial anisotropy for 4POPV and 6POPV is close to 0.4 in each case. 8POPV has a slightly lower initial anisotropy, although no noticeable decay on the time scale of our measurement. There may be some conformational disorder in the 8POPV chain since entropic effects become more important as the conjugated chains increase in length.[42,43] These observations are specific to POPV oligomers, that, like MEH-PPV, have a relatively simple manifold of electronic excited states. Other systems,[119] notably porphyrin oligomers, display more complicated anisotropy decays.[120]

In Figure 5a we plot the absorption spectrum calculated for a single PPV chain (chain C, Figure 1). Superimposed on that plot is the calculated inverse participation ratio, eq 8, for this chain. These calculations show that the spectroscopy of PPV-type polymers is dominated by disorder. That is, the conformational disorder breaks the chain up into effective chromophores, but because the excitation energies of these chromophores are widely distributed, the excitation is substantially localized despite the electronic coupling among subunits. Nonetheless, the electronic couplings among the subunits do yield slightly delocalized eigenstates. Previous work suggests that those eigenstates may localize to single conformational subunits via relaxation processes.[15,35,48,58] Such localization would affect the anisotropy by effectively rotating the transition dipole because the transition dipole vector of the exciton state differs from a localized state unless the chromophores are parallel. That is illustrated in Figure 5b, which plots the rotation of the transition dipole for each eigenstate on PPV chain C as it transforms from delocalized to localized. Clearly these rotations can be substantial, suggesting that localization may have a significant effect on the early time evolution of the pump−probe anisotropy. However, such a picture is purely for illustration, and serves to motivate the simulations described below.

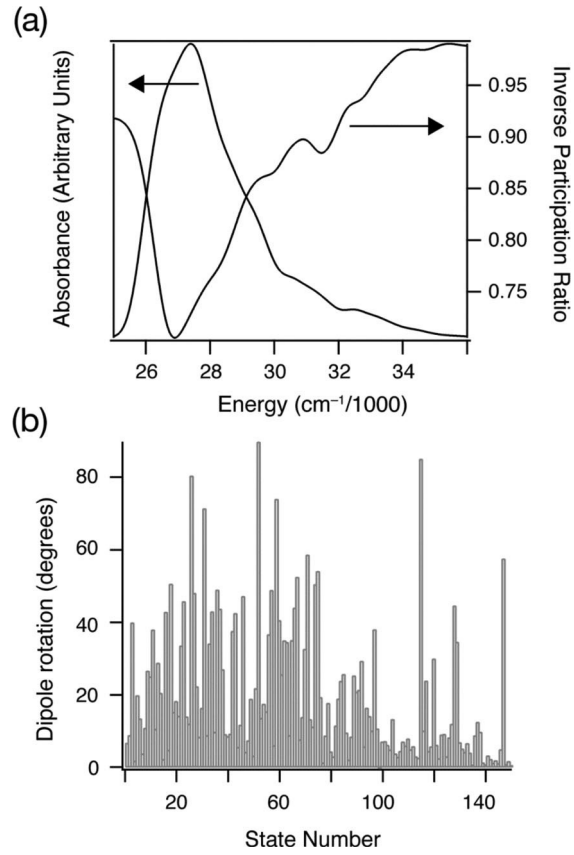

Figure 5. (a) Calculated absorption spectrum and inverse participation ratio for chain C. The inverse participation ratio is a measure of the extent of delocalization. 0 corresponds to completely delocalized. 1 is when the exciton is localized on a single subunit. The calculated spectra for all the chains are qualitatively similar (not shown). (b) The rotation of the dipole moment upon localization for chain C. The majority of the dipoles are rotated by fewer than 10° upon localization. However, a few chromophores may be rotated by as many as 85−90°.

The simulations based on eqs 9−13 and eq 6, showing the evolution of the early time (first 100 fs) emission spectra as a function of excitation wavelength, are reported in Figure 6. The shifting of early time fluorescence with excitation wavelength is consistent with that reported previously.[121] This shift has been found to be larger in polymers with broken conjugation,[35] in keeping with the larger proportion of shorter (blue) segments.

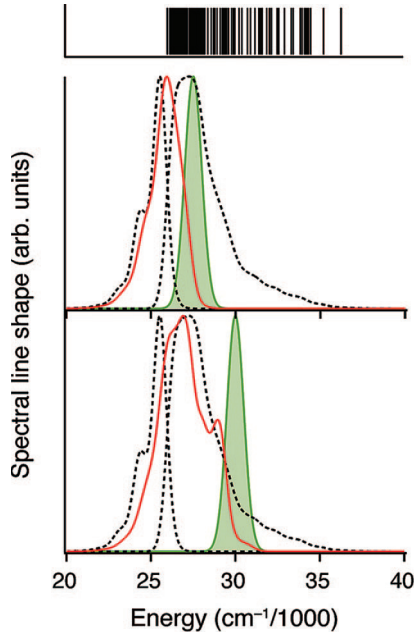

Figure 6. The effect of the excitation energy on the early time fluorescence. Calculated absorption and steady-state fluorescence spectra are shown in black for chain A. The excitation pulse is shown as a green Gaussian. The emission at 100 fs is shown in red. The early time fluorescence clearly changes depending on excitation energy. The density of states is shown at the top of the figure for reference. In the lower plot the abnormal shape of the early time fluorescence is due to the fact that even though the states nearest in energy to the excitation each contribute significantly to the early time fluorescence, the higher density of states further to the red sums to give a greater overall contribution, even though the contribution from each state is small. This accounts for the appearance of the peak at lower energies.

Notably, the population is predicted to shift very rapidly (over ~100 fs) to a low energy distribution via exciton relaxation. Additional spectral diffusion would be promoted by Förster-type energy transfer. As time progresses, a small time-dependent Stokes' shift is indeed observed in the simulations. It has previously been reported, based on time-resolved fluorescence measurements, that the 0−0 Stokes' shift changes by ~350 cm^{-1} during ~3 ns for samples of MEH-PPV and 180 cm^{-1} for PPV.[56] In ensemble measurements, the shape of the spectra change as well, reflecting the change in the relative contributions from the long and short chromophores with time. Intramolecular reorganization and energy transfer on a longer time scale are responsible for the remainder of the large apparent Stokes' shift observed in MEH-PPV[48] and other conjugated polymers. Again, this phenomenon is even more apparent in films, where interchain energy transfer dominates.[15,48] These relaxation processes are coupled with changes in transition dipole orientations that decay the anisotropy in the spirit of the simplistic model introduced in the preceding paragraph.

To gain a better understanding of the role that the microscopic conformation of each PPV chain plays in deciding the relaxation dynamics and anisotropy decay, simulations were performed where individual eigenstates were selectively excited. This is analogous to narrow line width excitation, whereas ultrashort pulse excitation generates a linear combination of these kinds of decay profiles. The results of the simulations demonstrate how disorder, even in single polymer chains, can blur details of the relaxation pathways and mechanism. Figure 7a shows examples of how the various types of effective chromophores that may be excited by the same laser pulse can lead to very different anisotropy decays. We find that excitons range from delocalized and strongly coupled cases that display fast anisotropy decays (case 1), to energetically isolated chromophores—a conformational subunit bordered by subunits of quite different energy—that are only very weakly coupled to others (case 3). These latter states exhibit little or no fast anisotropy decay. Interchain excitons can also be formed (case 2) where the conformational subunits that form the exciton are not adjacent along the chain but interact through-space.

Redistribution and relaxation of the exciton density (the probability distribution of finding a portion of the exciton on a site n at a given time) clearly decays the anisotropy even though the extent of spatial migration can be very small, as shown in Figure 7. This can happen on a rapid time scale (approximately <50 fs). As seen in Figure 7b for case 1, the excitation is quickly redistributed among the chromophores that comprise the collective electronic state when there are several contributing chromophores. These relaxation processes are enabled by overlapping wave function coefficients, as schematically illustrated in Figure 7c. Note that no significant geometrical distortion—free exciton equilibration enabled by coupling to nuclear modes—known as self-trapping is necessary to promote this relaxation. On the other hand, when the exciton is mostly localized on one conformational subunit, there is almost no decay in the anisotropy according to the exciton relaxation model, because that chromophore is coupled to others only very weakly.

The exciton relaxation as well as self-trapping can lead to localization of the exciton onto conformational subunits—the chromophores of the polymer—and subsequent dynamics involve hopping of that excitation among conformational subunits by a Förster-type EET. Förster-type EET involves the transfer of excitation from one chromophore to another and is promoted by weak electronic coupling between donor and acceptor (e.g., a dipole−dipole coupling between transition densities).[122] It therefore occurs in the opposite coupling regime to exciton relaxation, that is, EET occurs when the chromophores are strongly coupled to the bath relative to the electronic coupling between them. In contrast, exciton relaxation is mediated by weak exciton-bath coupling between eigenstates formed by relatively strong electronic coupling between the chromophores.

Consistent with the assignment of Herz and co-workers,[15] we postulate that the exciton relaxation precedes Förster-type EET and plays a role in localizing the excitation prior to long-range EET mediated by a Förster mechanism. That idea would be supported if there were a clear time scale separation between the two processes. Figure 8 shows calculated anisotropy decays for red-edge excitation conditions with realistic excitation pulse spectra but with the simplifying assumption that the excitation is instantaneous. Simulations for the three PPV chains shown in Figure 1 are compared. There appears to be a dependence on the radius of gyration of the polymer over longer time scales, but in the first 50 fs time window the decays are similar for each chain. The early time, rapid decay is the exciton relaxation and equilibration mediated by the bath of nuclear motions that couple to the electronic eigenstates, eqs 9–13. That relaxation among the eigenstates (see Figure 7) is seen as a net transition dipole rotation, and hence a decay in anisotropy. We anticipate that the exciton could be localized after the fastest component of this relaxation (in about 50−100 fs). That may occur by self-trapping (a self-consistent equilibration of exciton population density and nuclear coordinates, not considered in our model), or, as in the present simulations, simply by exciton relaxation to a bottleneck at longer subunits that tend to be more localized. This kind of localization by exciton relaxation is caused by the

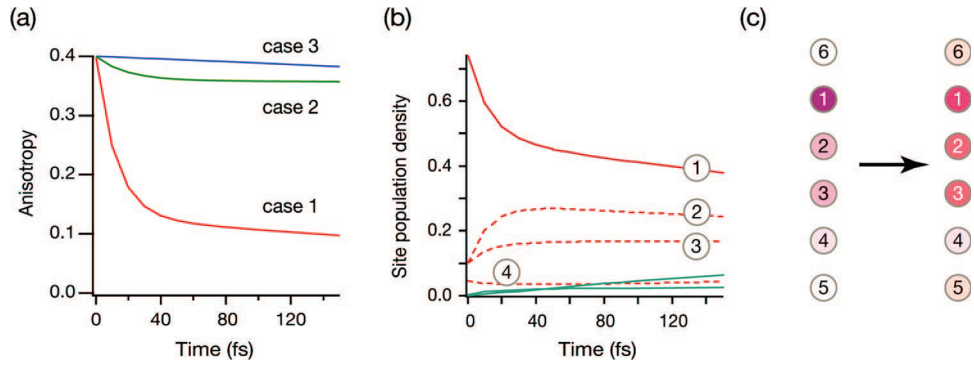

Figure 7. (a) Anisotropy decays for chain C when only one state is initially excited. Each trace corresponds to one of the following cases: Case 1, initially delocalized, strongly interacting exciton; Case 2, interchain exciton; Case 3, initially localized, weakly interacting exciton. (b) The redistribution of exciton density (between sites) for the initially delocalized exciton. Each trace corresponds to a different site/conformational subunit, *n*, on the polymer chain. (c) The anisotropy decay is caused by relaxation from one exciton state to another, indicated here similarly to the diagram in Figure 2. The shading on each site, or chromophore, (represented as a circle) illustrates the redistribution of occupation probability as the initial delocalized exciton state decays to populate five other exciton states.

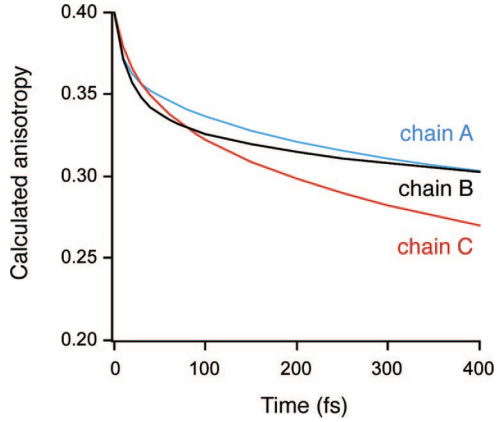

Figure 8. The simulated anisotropy decays based on exciton relaxation for the three chains shown in Figure 1.

strong disorder in site energies as a direct consequence of conformational disorder. By averaging over the calculated anisotropy during the initial 20−30 fs, we predict the initial anisotropy measured under excitation conditions similar to our experiment to be ∼0.37. That value compares well with the value of 0.36 we have measured for MEH-PPV.

Förster-type EET requires bath equilibration prior to each EET hop. It is unlikely that this can reasonably occur on the 10−20 fs time scale given that MEH-PPV is weakly coupled to the bath coordinates,[50] leading us to favor exciton relaxation for the <50 fs time window, whereas Förster energy migration will likely drive the anisotropy decay for times >50−100 fs. Perhaps, more realistically, competition between weak and strong coupling leads to the intermediate coupling regime for EET. Further evidence to support this time scale and mechanism separation comes from our previous use of the three-pulse photon echo peak shift (3PEPS) method that is very sensitive to spectral diffusion.[48,49]

Overview of Exciton Evolution and Dynamics in Conjugated Polymers. Upon light absorption by a conjugated polymer chain, excitation might be shared coherently among a few conformational subunits, thus forming exciton states. Our calculations suggest that these exciton states are substantially localized. However, although the extent of delocalization is small, the implications for the ultrafast evolution of the excited states are reasonably significant. Relaxation of these initially excited states has been found to be rapid, characterized by time scales of <50 fs, as observed clearly in the 3PEPS experiment[48,49,123] and fluorescence depolarization measurements.[15,35,124] The present work clarifies the likely origins of these ultrafast relaxation processes.

The net effect of relaxation among a high density of exciton states is to localize the excitation onto individual subunits. Dynamic effects might also assist excitation localization, whereby structural relaxation self-traps the excitation.[41,125,126] At time scales of ∼100 fs or more, significant geometric reorganizations and relaxation driven by low-frequency torsional motions, such as planarization of the conjugated π-system, take place.[58,127,128] On longer timescales yet, Förster-type EET becomes dominant, migrating the excitation through space to equilibrate on the lowest energy conformation subunits prior to fluorescence emission. In dilute solutions, intrachain energy transfer along isolated chains dominates, as there are relatively few chain−chain contacts.[129,130] Interchain energy transfer, which occurs predominantly in films, is faster and more efficient owing to the larger electronic couplings between conformational subunits.[15,39,48,59,131,132] Subsequent to EET, fluorescence emission emanates from a small subset of the entire ensemble of chromophores. This proposed timeline is summarized in Table 1.

Structural Reorganization after Photoexcitation. PPV oligomers have been predicted and observed to substantially change geometry after photoexcitation via a planarization.[58,127] Further evidence for geometrical relaxation has been found from studies of single poly(phenylene-ethynylene-butadiynylene) chains[133] as well as MEH-PPV.[134] Much previous work has demonstrated the importance of torsional motions on the spectroscopy of conjugated polymers and oligomers, most obviously in the asymmetry between absorption and PL spectra.[6,45,49,135] High-frequency modes might also play a role in relaxation processes. These kinds of dynamic effects were not considered in the relaxation model used in the present work.

The large geometry change associated with torsional relaxation, which is also very likely upon the excitation energy of MEH-PPV, lowers the mean free energy and could contribute to self-trapping if it were rapid enough (i.e., strongly coupled to the exciton).[58,136] However, planarization of conjugated oligomers is reported to occur on the >100 fs time scale,[127] which therefore occurs subsequently to exciton relaxation, consistent with our postulated time sequence of excited-state dynamics, Table 1. Furthermore, it is not clear how to estimate the coupling strength of these modes to the exciton because they have zero displacement. The anisotropy decays for the

TABLE 1: Evolution of Excitation in Disordered Conjugated Polymers

process	relevant timescale	effect on anisotropy?
relaxation through manifold of exciton states	<50 fs	Spatial and energetic changes small. Decays anisotropy and gives a particularly rapid decay in 3PEPS[a] data. Rapidly localizes excitation in PPV because of the dominance of conformational disorder.
self-trapping of exciton caused by geometry distortion	~100 fs	Localizes excitation to individual subunits by geometrical and/or bath equilibration. May involve planarization of the chromophores.
interchain EET (in films, nanoparticles, and aggregates)	ps to 10s of ps	Significant energetic and spatial migration. Large depolarization.
intrachain EET	10s to 100s of ps	
fluorescence emission (exciton recombination)	~1 ns	From subset of ensemble corresponding to the red-most chromophores.

[a] 3PEPS (three-pulse photon echo peak shift) measures the time scales over which loss of the initial electronic frequency distribution occurs. See refs.[47−49]

POPV oligomers presented in Figure 4 support the hypothesis that torsional modes are not involved in the ultrafast anisotropy decay, at least with respect to isolated chromophores. This remains an issue for debate, with others ascribing self-trapping to coupling to these modes[42,43,58,128] rather than higher frequency modes.

It has been proposed that the rate of EET is affected by torsional relaxation on a picosecond time scale.[137] Westenhoff et al. demonstrate that the exciton size increases upon torsional relaxation in polythiophenes and that accounting for this is necessary to correctly simulate the energy transfer dynamics. Using a site-selective experiment where EET cannot contribute, they attribute a red shift in the PL to this relaxation. The red shift is not observed in samples where the torsions are blocked.[137] The reorganization associated with some intramolecular modes is likely to occur on a time scale similar to that of energy transfer in MEH-PPV as well.[34] In MEH-PPV, however, the importance of these effects may be obscured or diminished by the larger conformational disorder and disorder-related localization, like that considered in the present work.[32]

Exciton Relaxation and the Importance of Disorder. Owing to the significant structural disorder in PPV chains, neighboring exciton states can have very different dipole transition moment vectors, meaning that exciton relaxation between those states can be accompanied by rapid depolarization. Localization onto a single conformational subunit will have a similar depolarizing effect. Using models based on eqs 9−13 we found that the evolution of the excited states are strikingly strongly influenced by the degree of disorder present in the polymer chain. This observation is the focus of this section.

As shown in Figure 6, the calculated early time-fluorescence derives from a subset of the ensemble of states that is near in energy to that of the excitation source. That is, absorption and fluorescence are from nearly the same set of chromophores; there is little spectral diffusion. Nonetheless, the anisotropy can change greatly on this short time scale, as shown in Figures 7 and 8, without requiring a large average energy change. These same relaxation processes are likely to be responsible for the ultrafast 3PEPS decay reported for these same polymers.[48,49]

In practice, the averaging implicit in an ensemble experiment largely washes away the conformation-dependence. Nonetheless, it is useful to compare simulations for the representative chains A, B, and C as a function of their radii of gyration, Figure 8. The different exciton relaxation dynamics found for these chains is a result of the tendency for particular types of chain conformations to contain certain varieties of chromophores more often. The chain with the largest radius of gyration, that is, the most extended conformation, is found to have the slowest anisotropy decay on average. It contains a broad distribution of chromophore lengths (conformational subunits), meaning that it is unlikely for two similar chromophores to lie in close proximity. The composition of exciton states is dictated not only by electronic coupling among chromophores, but also by their energy mismatch. That is because, when the chromophores are nondegenerate, the mixing coefficients in the exciton wave function are approximately proportional to V/A (according to perturbation theory), where V is the electronic coupling and A is the energy mismatch. The smallest radius chain contains a higher percentage of shorter chromophores. Because these chromophores are more common, they are more likely to lie adjacent to each other on the chain. The result is that they can couple effectively and form a set of states through which excitation can relax efficiently.

Although subtleties relating chain conformation to anisotropy decay may often become lost in ensemble measurements, the work on fluorescence depolarization by Grage et al. found an anisotropy−decay dependence on chain conformation.[32] A key result of the present work is that it is not only spatial proximity of conformational subunits that determines mixing of chromophore excited states to form excitons but also their energetic compatibility. The fastest exciton relaxation, and thereby anisotropy decay, processes are enabled by relaxation to lower energy states formed by shared electronic excitation on proximate conformational subunits of similar size. Hence, conformational disorder plays a deciding role in intrachain exciton formation and the fastest relaxation processes occurring after photoexcitation by disrupting the energetic compatibility between neighboring chromophores along the polymer backbone.

Conclusions

There has been much discussion as to the nature of the ultrafast decay component observed in polarization anisotropy and 3PEPS (three-pulse photon echo peak shift) experiments on conjugated polymers.[15,35,48−50] The complex photophysical response of conjugated polymers makes it difficult to ascribe this decay to any single phenomenon. Indeed, multiple competing processes likely contribute to varying degrees, including localization or self-trapping of the excitation, relaxation within the exciton manifold, or polaron formation and recombination.[108] Evidently, the excited-state evolution over the first 100 fs is complicated and involves the interplay among strong and weak coupling of excited states.[118,138] We conclude, however, that disorder is both a defining and limiting characteristic of PPV-family conjugated polymers.

Overall, we have presented the point of view that relaxation through a manifold of subtly delocalized exciton states on isolated PPV-type chains can lead to rapid depolarization of

the anisotropy. Such ultrafast anisotropy decay has previously been reported by others, including Herz and co-workers.[15] The exciton relaxation we have modeled is not necessarily accompanied by large energetic or spatial migration of the exciton but is a consequence of the disorder inherent in polymer chains. Simulations and calculations were necessary to obtain these insights because the subtleties of such effects are hidden by the large degree of disorder in the ensemble that is probed by experiment. In fact, even single molecule calculations were affected by the microscopic nature of the numerous chromophores on a single polymer chain. A general result discovered from the chain-by-chain simulations of spectroscopy is that energetic disorder, caused by conformational disorder, plays a deciding role in the photophysics. In particular, disorder in the excitation energies of conformational subunits along the PPV chain greatly limits delocalization and concomitantly suppresses relaxation pathways because of the substantial energy mismatches between neighboring subunits.

Acknowledgment. The Natural Sciences and Engineering Research Council of Canada is gratefully acknowledged for support of this research. G.D.S. acknowledges the support of an E. W. R. Steacie Memorial Fellowship. We thank Professor Herbert Meier, Mainz (Germany), in whose group the POPV molecules were synthesized. The work in Mons was supported by the European Commission through the EC STREP project MODECOM (NMP-CT-2006-016434), the Belgian National Science Foundation (FNRS), and the Belgian Federal Science Policy Office in the framework of the Interuniversity Attraction Pole IAP 6/27 Program of the Belgian Federal Government "Functional supramolecular systems (FS2)". D.B. is a Research Associate of the FNRS. E.R.B. acknowledges the support of the National Science Foundation (CHE-0712981), the Robert A. Welch foundation (E-1337), and the J. S. Guggenheim Foundation. J.G. is a "Ramon y Cajal" fellow of the Spanish Ministry for Education and Science, Spain.

Supporting Information Available: Supplementary experimental and theoretical results are plotted. The geometry and Hamiltonian for each of the PPV chains A–C are also provided. This material is available free of charge via the Internet at http://pubs.acs.org.

References and Notes

(1) *Semiconducting polymers: Chemistry, Physics and Engineering*, 2 ed.; Hadziioannou, G.; Malliaras, G. G., Eds.; Wiley-VCH: Weinheim, 2007.

(2) Bullot, J.; Dulieu, B.; Lefrant, S. *Synth. Met.* **1993**, *61*, 211.

(3) Möhlmann, G. R. *Synth. Met.* **1994**, *67*, 77.

(4) Baigent, D. R.; Greenham, N. C.; Grüner, J.; Marks, R. N.; Friend, R. H.; Moratti, R. C.; Holmes, A. B. *Synth. Met.* **1994**, *67*, 3–10.

(5) Oelkrug, D.; Tompert, A.; Egelhaaf, H.-J.; Hanack, M.; Steinhuber, E.; Hohloch, M.; Meier, H.; Stalmach, U. *Synth. Met.* **1996**, *83*, 231–237.

(6) Oelkrug, D.; Tompert, A.; Gierschner, J.; Egelhaaf, H.-J.; Hanack, M.; Hohloch, M.; Steinhuber, E. *J. Phys. Chem. B* **1998**, *102*, 1902.

(7) Egelhaaf, H.-J.; Lüer, L.; Tompert, A.; Bäuerle, P.; Müllen, K.; Oelkrug, D. *Synth. Met.* **2000**, *115*, 63–68.

(8) Birckner, E.; Grimmt, U. W.; Hartmann, A.; Pfeiffer, S.; Tillmann, H.; Hörhold, H.-H. *J. Fluor.* **1998**, *8*, 73.

(9) Son, S.; Dodabalapur, A.; Lovinger, A. J.; Galvin, M. E. *Science* **1995**, *269*, 376–378.

(10) Schwartz, B. J. *Annu. Rev. Phys. Chem.* **2003**, *54*, 141–72.

(11) Heun, S.; Mahrt, R. F.; Greiner, A.; Lemmer, U.; Bässler, H.; Halliday, D. A.; Bradley, D. D. C.; Burn, P. L.; Holmes, A. B. *J. Phys.: Condens. Matter* **1993**, *5*, 247–260.

(12) Chang, R.; Hsu, J. H.; Fann, W. S.; Liang, K. K.; Chang, C. H.; Hayashi, M.; Yu, J.; Lin, S. H.; Chang, E. C.; Chuang, K. R.; Chen, S. A. *Chem. Phys. Lett.* **2000**, *317*, 142–152.

(13) Yu, J.; Hu, D.; Barbara, P. F. *Science* **2000**, *289*, 1327–1330.

(14) Samuel, I. D. W.; Crystall, B.; Rumbles, G.; Burn, P. L.; Holmes, A. B.; Friend, R. H. *Chem. Phys. Lett.* **1993**, *213*, 472.

(15) Chang, M. H.; Frampton, M. J.; Anderson, H. L.; Herz, L. M. *Phys. Rev. Lett.* **2007**, *98*, 027402.

(16) *Primary Excitations in Conjugated Polymers: Molecular Exciton versus Semiconductor Band Model*; Sariciftci, N. S., Ed.; World Scientific: Singapore, 1997.

(17) Lécuiller, R.; Berréhar, J.; Ganière, J. D.; Lapersonne-Meyer, C.; Lavallard, P.; Schott, M. *Phys. Rev. B* **2002**, *66*, 125205.

(18) Dubin, F.; Melet, R.; Barisien, T.; Grousson, R.; Legrand, L.; Schott, M.; Voliotis, V. *Nat. Phys.* **2006**, *2*, 32.

(19) Bässler, H. *Site-Selective Fluorescence Spectroscopy of Polymers*; Elsevier: Amsterdam, 1989.

(20) Mahrt, R. F.; Bässler, H. *Synth. Met.* **1991**, *45*, 107–117.

(21) Harrison, N. T.; Baigent, D. R.; Samuel, I. D. W.; Friend, R. H.; Grimsdale, A. C.; Moratti, S. C.; Holmes, A. B. *Phys. Rev. B* **1996**, *53*, 15815.

(22) Schweizer, K. S. *J. Chem. Phys.* **1986**, *85*, 1156–1175.

(23) Schreiber, M.; Abe, S. *Synth. Met.* **1993**, *55*, 50–55.

(24) Lhost, O.; Brédas, J. L. *J. Chem. Phys.* **1992**, *96*, 5279–5288.

(25) Soos, Z. G.; Ramasesha, S.; Galvao, D. S.; Etemad, S. *Phys. Rev. B* **1993**, *47*, 1742.

(26) Galvao, D. S.; Soos, Z. G.; Ramesesha, S.; Etemad, S. *J. Chem. Phys.* **1993**, *98*, 3016–3021.

(27) Yaliraki, S. N.; Silbey, R. J. *J. Chem. Phys.* **1996**, *104*, 1245–1253.

(28) Kohler, B. E.; Samuel, I. D. W. *J. Chem. Phys.* **1995**, *103*, 6248–6252.

(29) Kohler, B. E.; Woehl, J. C. *J. Chem. Phys.* **1995**, *103*, 6253–6256.

(30) Cornil, J.; dos Santos, D. A.; Crispins, X.; Silbey, R. J.; Brédas, J. L. *J. Am. Chem. Soc.* **1998**, *120*, 1289–1299.

(31) Karabunarliev, S.; Baumgarten, M.; Müllen, K. *J. Phys. Chem. A* **2000**, *104*, 8236.

(32) Grage, M. M.-L.; Wood, P. W.; Ruseckas, A.; Pullerits, T.; Mitchell, W.; Burn, P. L.; Samuel, I. D. W.; Sundström, V. *J. Chem. Phys.* **2003**, *118*, 7644–7650.

(33) Gaab, K. M.; Bardeen, C. J. *J. Phys. Chem. A* **2004**, *108*, 10801.

(34) Chang, R.; Hayashi, M.; Lin, S. H.; Hsu, J.-H.; Fann, W. S. *J. Chem. Phys.* **2001**, *115*, 4339–4348.

(35) Ruseckas, A.; Wood, P.; Samuel, I. D. W.; Webster, G. R.; Mitchell, W. J.; Burn, P. L.; Sundström, V. *Phys. Rev. B* **2005**, *72*, 115214.

(36) Herz, L. M.; Silva, C.; Grimsdale, A. C.; Müllen, K.; Phillips, R. T. *Phys. Rev. B* **2004**, *70*, 165207.

(37) Vaughan, H. L.; Dias, F. M. B.; Monkman, A. P. *J. Chem. Phys.* **2005**, *122*, 014902.

(38) Hennebicq, E.; Deleener, C.; Brédas, J. L.; Scholes, G. D.; Beljonne, D. *J. Chem. Phys.* **2006**, *125*, 054901.

(39) Hennebicq, E.; Pourtois, G.; Scholes, G. D.; Herz, L. M.; Russel, D. M.; Silva, C.; Müllen, K.; Brédas, J. L.; Beljonne, D. *J. Am. Chem. Soc.* **2005**, *127*, 4744–4762.

(40) Beenken, W. J. D.; Lischka, H. *J. Chem. Phys.* **2005**, *123*, 144311.

(41) Beenken, W. J. D.; Pullerits, T. *J. Phys. Chem. B* **2004**, *108*, 6164–6169.

(42) Liu, L. T.; Yaron, D.; Sluch, M. I.; Berg, M. A. *J. Phys. Chem. B* **2006**, *110*, 18844.

(43) Liu, L. T.; Yaron, D.; Berg, M. A. *J. Phys. Chem. C* **2007**, *111*, 5770.

(44) Wells, N. P.; Blank, D. A. *Phys. Rev. Lett.* **2008**, *100*, 086403.

(45) Gierschner, J.; Mack, H.-G.; Lüer, L.; Oelkrug, D. *J. Chem. Phys.* **2002**, *116*, 8596–8609.

(46) Bässler, H.; Schweitzer, B. *Acc. Chem. Res.* **1999**, *32*, 173–182.

(47) Scholes, G. D.; Rumbles, G. *Nat. Mater.* **2006**, *5*, 683.

(48) Dykstra, T. E.; Kovalevskij, V.; Yang, X.; Scholes, G. D. *Chem. Phys.* **2005**, *318*, 21–32.

(49) Yang, X.; Dykstra, T. E.; Scholes, G. D. *Phys. Rev. B* **2005**, *71*, 045203.

(50) Scholes, G. D.; Larsen, D. S.; Fleming, G. R.; Rumbles, G.; Burn, P. L. *Phys. Rev. B* **2000**, *61*, 13670.

(51) Rothberg, L. J.; Yan, M.; Galvin, M. E.; Kwock, E. W.; Miller, T. M.; Papadimitrakopoulos, F. *Synth. Met.* **1996**, *80*, 41.

(52) Yan, M.; Rothberg, L. J.; Kwok, E. W.; Miller, T. M. *Phys. Rev. Lett.* **1995**, *75*, 1992.

(53) Leng, J. M.; Jeglinski, S.; Wei, X.; Brenner, R. E.; Vardeny, Z. V.; Guo, F.; Mazumdar, S. *Phys. Rev. Lett.* **1994**, *72*, 156.

(54) Österbacka, R.; Wohlgenannt, M.; Chinn, D.; Vardeny, Z. V. *Phys. Rev. B* **1999**, *60*, 11253.

(55) Lim, S.-H.; Bjorklund, T. G.; Gaab, K. M.; Bardeen, C. J. *J. Chem. Phys.* **2002**, *117*, 454.

(56) Bjorklund, T. G.; Lim, S.-H.; Bardeen, C. J. *J. Phys. Chem. B* **2001**, *105*, 11970.

(57) Heller, C. M.; Campbell, I. H.; Laurich, B. K.; Smith, D. L.; Bradley, D. D. C.; Burn, P. L.; Ferrais, J. P.; Müllen, K. *Phys. Rev. B* **1996**, *54*, 5516.
(58) Tretiak, S.; Saxena, A.; Martin, R. L.; Bishop, A. R. *Phys. Rev. Lett.* **2002**, *89*, 097402.
(59) Beljonne, D.; Pourtois, G.; Silva, C.; Hennebicq, E.; Herz, L. M.; Friend, R. H.; Scholes, G. D.; Setayesh, S.; Müllen, K.; Brédas, J. L. *Proc. Nat. Acad. Sci.* **2002**, *99*, 10982–10987.
(60) Hartree, D. R. *Proc. Cambridge Phil. Soc. Math. Phys. Sci.* **1928**, *24*, 328.
(61) Dewar, M. J. S.; Zoesbisch, E. G.; Healy, E. F.; Stewart, J. J. P. *J. Am. Chem. Soc.* **1995**, *107*, 3702.
(62) Rissler, J.; Bässler, H.; Gebhard, F.; Schwerdtfeger, P. *Phys. Rev. B* **2001**, *64*, 045122.
(63) Møller, C.; Plesset, M. S. *Phys. Rev.* **1934**, *46*, 618.
(64) Pople, J. A.; Beveridge, D. L.; Dobosch, P. A. *J. Chem. Phys.* **1967**, *47*, 2026.
(65) Fock, V. Z. *Phys.* **1930**, *61*, 126.
(66) Zerner, M. C.; Loew, G. H.; Kichner, R. F.; Mueller-Westerhoff, V. T. *J. Am. Chem. Soc.* **1980**, *102*, 5279.
(67) Ridley, J.; Zerner, M. C. *Theoret. Chim. Acta* **1973**, *32*, 111.
(68) Mataga, N.; Nishimoto, K. *Z. Phys. Chem.* **1957**, *13*, 140.
(69) Pariser, R.; Parr, R. *J. Chem. Phys.* **1953**, *21*, 767.
(70) Cornil, J.; Beljonne, D.; Friend, R. H.; Brédas, J. L. *Chem. Phys. Lett.* **1994**, *223*, 82.
(71) Marguet, S.; Markovitsi, D.; Millié, P.; Sigal, H.; Kumar, S. *J. Phys. Chem. B* **1998**, *102*, 4697.
(72) Krueger, B. P.; Scholes, G. D.; Fleming, G. R. *J. Phys. Chem. B* **1998**, *102*, 5378–5386.
(73) Claudio, G. C.; Bittner, E. R. *J. Chem. Phys.* **2001**, *115*, 9585.
(74) Claudio, G. C.; Bittner, E. R. *J. Phys. Chem. A* **2003**, *107*, 7092.
(75) Scholes, G. D.; Fleming, G. R. *J. Phys. Chem. B* **2000**, *104*, 1854–1868.
(76) Myers, A. B. *J. Opt. Soc. Am. B* **1990**, *7*, 1665–1672.
(77) Myers, A. B. *J. Raman Spectrosc.* **1997**, *28*, 389–401.
(78) Mukamel, S. *Principles of Nonlinear Optical Spectroscopy*; Oxford University Press: New York, 1995.
(79) Fidder, H.; Knoester, J.; Wiersma, D. A. *J. Chem. Phys.* **1991**, *95*, 7880.
(80) Heijs, D. J.; Malyshhev, V. A.; Knoester, J. *Phys. Rev. Lett.* **2005**, *95*, 177402.
(81) Bednarz, M.; Malyshev, V. A.; Knoester, J. *J. Chem. Phys.* **2002**, *117*, 6200–6213.
(82) Didraga, C.; Malyshev, V. A.; Knoester, J. *J. Phys. Chem. B* **2006**, *110*, 18818–18827.
(83) Bednarz, M.; Malyshev, V. A.; Knoester, J. *J. Chem. Phys.* **2003**, *91*, 217401.
(84) Kubo, R. *Adv. Chem. Phys.* **1969**, *15*, 101–127.
(85) Sue, J.; Yan, Y. J.; Mukamel, S. *J. Chem. Phys.* **1986**, *85*, 462–474.
(86) Samuel, I. D. W.; Rumbles, G.; Collison, C. J. *Phys. Rev. B* **1995**, *52*, 11573.
(87) Grozema, F. C.; Siebbeles, L. D. A.; Gelinck, G. H.; Warman, J. M. *Top. Curr. Chem.* **2005**,
(88) Cross, A. J.; Fleming, G. R. *Biophys. J.* **1984**, *46*, 45–56.
(89) Gochanour, C. R.; Fayer, M. D. *J. Phys. Chem.* **1981**, *85*, 1989.
(90) Lakowicz, J. R. *Principles of Fluorescence Spectroscopy*; Plenum Press: New York, 1983.
(91) Wilhelm, T.; Piel, J.; Riedle, E. *Opt. Lett.* **1997**, *22*, 1494.
(92) Stalmach, U.; Kolshorn, H.; Brehm, I.; Meier, H. *Liebigs Annalen* **1996**, 1449–1456.
(93) Zaushitsyn, Y.; Jespersen, K. G.; Valkunas, L.; Sundström, V.; Yartsev, A. *Phys. Rev. B* **2007**, *75*, 195201.
(94) Martini, I. B.; Smith, A. D.; Schwartz, B. J. *Phys. Rev. B* **2004**, *69*, 035204.
(95) De Schryver, F. C.; Vosch, T.; Cotlet, M.; Van Der Auweraer, M.; Müllen, K.; Hofkens, J. *Acc. Chem. Res.* **2005**, *38*, 514–522.
(96) McClain, W. M. *J. Chem. Phys.* **1972**, *57*, 2264–2272.
(97) Wagnière, G. *J. Chem. Phys.* **1982**, *76*, 473–480.
(98) Scholes, G. *J. Chem. Phys.* **2004**, *121*, 10104–10110.
(99) Goodson, T. *Annu. Rev. Phys. Chem.* **2005**, *56*, 581–603.
(100) Andrews, D. L.; Blake, N. P. *J. Phys. A: Math. Gen.* **1989**, *22*, 49–60.
(101) Andrews, D. L.; Thirunamachandran, T. *J. Chem. Phys.* **1977**, *67*, 5026.
(102) Scholes, G. D.; Kim, J.; Wong, C. Y. *Phys. Rev. B* **2006**, *73*, 195325.
(103) Joo, T.; Jia, Y.; Yu, J.-Y.; Lang, M. J.; Fleming, G. R. *J. Chem. Phys.* **1996**, *104*, 6089–6108.
(104) Frankevich, E. L.; Lymarev, A. A.; Sokolik, I.; Karasz, F. E.; Baughman, R.; Hörhold, H. H. *Phys. Rev. B* **1992**, *46*, 320.
(105) Lee, C. H.; Yu, G.; Heeger, A. J. *Phys. Rev. B* **1993**, *47*, 15543.
(106) Conwell, E. M.; Mizes, H. A. *Phys. Rev. B* **1995**, *51*, 6953.
(107) Lane, P. A.; Wei, X.; Vardeny, Z. V. *Phys. Rev. B* **1997**, *56*, 4626.
(108) Kraabel, B.; McBranch, D.; Sariciftci, N. S.; Moses, D.; Heeger, A. J. *Phys. Rev. B* **1994**, *50*, 18543–18552.
(109) Rothberg, L.; Jedju, T. M.; Townsend, P. D.; Etemad, S.; Baker, G. L. *Phys. Rev. Lett.* **1990**, *65*, 100–103.
(110) Arkhipov, V. I.; Bässler, H. *Phys. Stat. Solidi A* **2004**, *201*, 1152–1187.
(111) An, Z.; Wu, C. Q.; Sun, X. *Phys. Rev. Lett.* **2004**, *93*, 216407.
(112) Moses, D.; Dogarlu, A.; Heeger, A. J. *Chem. Phys. Lett.* **2000**, *316*, 356–360.
(113) Sheng, C. X.; Tong, M.; Singh, S.; Vardeny, Z. V. *Phys. Rev. B* **2007**, *75*, 085206.
(114) Greenham, N. C.; Samuel, I. D. W.; Hayes, G. R.; Phillips, R. T.; Kessener, Y. A. R. R.; Moratti, S. C.; Holmes, A. B.; Friend, R. H. *Chem. Phys. Lett.* **1995**, *241*, 89–96.
(115) Silva, C.; Russell, D. M.; Dhoot, A. S.; Herz, L. M.; Daniel, C.; Greenham, N. C.; Arias, A. C.; Setayesh, S.; Müllen, K.; Friend, R. H. *J. Phys.: Condens. Matter* **2002**, *14*, 9803–9824.
(116) Hendry, E.; Schins, J. M.; Candeias, L. P.; Siebbeles, L. D. A.; Bonn, M. *Phys. Rev. Lett.* **2004**, *92*.
(117) Miranda, P. B.; Moses, D.; Heeger, A. J. *Phys. Rev. B* **2004**, *70*, 085212.
(118) Collini, E.; Scholes, G. D. *Science*, **2008**, in press.
(119) Smith, E.; Farrow, D.; Jonas, D. *J. Chem. Phys.* **2005**, *123*, 044102.
(120) Chang, M. H.; Hoffmann, M.; Anderson, H. L.; Herz, L. M. *J. Am. Chem. Soc.* **2008**, *130*, 10171–10178.
(121) Gaab, K. M.; Bardeen, C. J. *J. Phys. Chem. B* **2004**, *108*, 4619–4626.
(122) Scholes, G. D. *Annu. Rev. Phys. Chem.* **2003**, *54*, 57–87.
(123) Yang, M.; Agarwal, R.; Fleming, G. R. *J. Photochem. Photobiol. A* **2001**, *142*, 107–119.
(124) Ruseckas, A.; Samuel, I. D. W. *Phys. Stat. Solidi C* **2006**, *3*, 263–266.
(125) Karabunarliev, S.; Bittner, E. B. *J. Chem. Phys.* **2003**, *118*, 4291–4296.
(126) Timpmann, K.; Rätsep, M.; Hunter, C. N.; Freiberg, A. *J. Phys. Chem. B* **2004**, *108*, 10581–10588.
(127) Wong, K. S.; Wang, H. X.; Lanzani, G. *Chem. Phys. Lett.* **1998**, *288*, 59–64.
(128) Franco, I.; Tretiak, S. *J. Am. Chem. Soc.* **2004**, *126*, 12130–12140.
(129) Nesterov, E. E.; Zhu, Z.; Swager, T. M. *J. Am. Chem. Soc.* **2005**, *127*, 10083–10088.
(130) Nguyen, T.-Q.; Wu, J.; Doan, V.; Schwartz, B. J.; Tolbert, S. H. *Science* **2000**, *288*, 652–6.
(131) Beljonne, D.; Pourtois, G.; Shuai, Z.; Hennebicq, E.; Scholes, G. D.; Brédas, J. L. *Synth. Met.* **2003**, *137*, 1369–1371.
(132) Beljonne, D.; Hennebicq, E.; Daniel, C.; Herz, L. M.; Silva, C.; Scholes, G. D.; Hoeben, F. J. M.; Jonkheijm, P.; Schenning, A. P. H. J.; Meskers, S. C. J.; Phillips, R. T.; Friend, R. H.; Meijer, E. W. *J. Phys. Chem. B* **2005**, *109*, 10594–10604.
(133) Walter, M. J.; Lupton, J. M.; Becker, K.; Feldmann, J.; Gaefke, G.; Höger, S. *Phys. Rev. Lett.* **2007**, *98*, 137401.
(134) Pullerits, T.; Mirzov, O.; Scheblykin, I. G. *J. Phys. Chem. B* **2005**, *109*, 19099–19107.
(135) Rothberg, L. J. In *Semiconducting Polymers: Chemistry, Physics, and Engineering*, 2nd Ed.; Hadziioannu, G.; Malliaras, G. G., Eds.; Wiley-VCH: Weinheim, 2007, p 179.
(136) Wexler, D.; Kochendoerfer, G. G.; Mathies, R. A. In *Femtochemistry and Femtobiology: Ultrafast Reaction Dynamics at Atomic Scale Resolution*; Imperial College Press: London, 1997,
(137) Westenhoff, S.; Beenken, W.; Friend, R. H.; Greenham, N. C. *Phys. Rev. Lett.* **2006**, *166804*.
(138) Scholes, G. D.; Ghiggino, K. P. *J. Chem. Phys.* **1994**, *101*, 1251–1261.

JP807249B